

Coverage-dependent adsorption, dissociation and aggregation of H₂O on the clean and pre-adsorbed oxygen Cu(111) surface: A DFT study



Xiaobin Hao^a, Riguang Zhang^{a,b,*}, Leilei He^b, Zaixing Huang^b, Baojun Wang^a

^a Key Laboratory of Coal Science and Technology of Ministry of Education and Shanxi Province, Taiyuan University of Technology, Taiyuan 030024, Shanxi, PR China

^b Department of Chemical and Petroleum Engineering, The University of Wyoming, Laramie, WY 82071, USA

ARTICLE INFO

Article history:

Received 18 September 2017

Received in revised form 6 November 2017

Accepted 24 November 2017

Keywords:

H₂O

Cu(111)

Adsorption

Dissociation

Aggregation

ABSTRACT

Density functional theory calculations have been employed to investigate the adsorption and dissociation of H₂O, as well as the aggregation of H₂O over the clean and pre-adsorbed oxygen Cu(111) surface at different coverage. As the coverage increases, the adsorption ability of H₂O, OH, H and O species becomes gradually weaker, H₂O dissociation becomes more unfavorable on both the clean and pre-adsorbed oxygen Cu(111) surface. H₂O desorption is more favorable than its dissociation on the clean Cu(111) surface at the different coverage due to the weak physical interaction between H₂O molecule and Cu surface. However, on the pre-adsorbed oxygen Cu(111) surface, the adsorbed oxygen atom promotes H₂O dissociation at different coverage, and H₂O prefers to be dissociated instead of its desorption at the coverage below 0.50 ML. For H₂O aggregation over Cu(111) surface, as the number of H₂O molecule increases, the aggregation becomes easier due to the stronger hydrogen-bond interaction among different adsorbed H₂O molecules, while the interaction between (H₂O)_n and Cu surface becomes weaker.

© 2017 Elsevier B.V. All rights reserved.

1. Introduction

The water-gas-shift (WGS) reaction, H₂O + CO → H₂ + CO₂, is an important and widely studied reaction system on Cu-based catalysts [1–4]. This reaction plays a key role not only in the production of high purity hydrogen for fuel cells [5,6], but also in the synthesis of ammonia and methanol [7,8]. It is well known that the interaction between H₂O and Cu metal is very important to understand WGS reaction mechanism, and H₂O dissociation is usually thought to be the rate-determining step of WGS reaction [9,10]. Meanwhile, the studies about the adsorption and dissociation of H₂O on Cu metal are also useful to understand the phenomena like corrosion, electrolysis, fuel cells, and biotechnologies, and so on [11,12]. Thus, the detailed knowledge of H₂O adsorption and dissociation on Cu surface is significant for the comprehensive understanding these applications.

Nowadays, great efforts have been devoted to the experimental and theoretical studies on the adsorption and dissociation of H₂O on Cu surface. A larger number of studies have demonstrated that the single H₂O molecule prefers to adsorb at the top site on

Cu surface, where the plane of H₂O molecule is nearly parallel to the Cu surface [13–17]. In the reported experiments, Roberts et al. [18] investigated the interaction of H₂O with the clean Cu(111) surface using X-ray photoelectron spectroscopy, suggesting that H₂O adsorbs on Cu(111) surface at 80 K, while it desorbs from Cu(111) surface at about 140 K. Taylor Campbell et al. [19] presented an activation barrier of 83.9 kJ mol⁻¹ for H₂O dissociation in WGS reaction by kinetic measurements combined with UHV surface analysis. After heating Cu(110) surface with adsorbed H₂O to T > 200 K, OH species have been detected using the infrared reflection absorption spectroscopy (IRAS) and electron energy loss spectroscopy (EELS) [20,21]. Taylor's studies [22] found that the orbitals of H₂O are engaged much more weakly with the frontier orbitals on Cu surface. Density functional theory (DFT) studies by Chen et al. [23] calculated the adsorption of a single H₂O on a p(3 × 3) Cu(111) and (100) surfaces corresponding to the coverage of 0.11 ML, and a corrugated p(2 × 2) Cu(110) surface at 0.25 ML, as well as the stepped p(1 × 2) Cu(211) and (221) surface at 0.50 ML, suggesting that H₂O molecule tends to weakly bind to the top site with the molecular plane basically parallel to the substrate surface. Ren et al. [24] calculated the adsorption and dissociation of a single H₂O molecule on a p(2 × 2) Cu(110) surface, suggesting that H₂O prefers to be adsorbed at the top site with the plane of H₂O molecule lying flat, and the dissociation of H₂O is impossible due to the high barrier. Jiang et al.

* Corresponding author at: No. 79 Yingze West Street, Taiyuan 030024, PR China.
E-mail address: zhangriguang@tyut.edu.cn (R. Zhang).

[25] theoretically investigated the effects of surface charge on the adsorption and dissociation of a single H₂O on a $p(3 \times 3)$ Cu(111) surface corresponding to the coverage of 0.11 ML. The DFT studies by Fajin et al. [26] showed that the presence of step site benefits for a single H₂O dissociation into OH and H while OH cannot further dissociate or disproportionate over Cu(321) surface. Rowley et al. [27] studied the adsorption of a single H₂O molecule on Cu₁₀ and Cu₁₈ cluster models using *ab-initio* methods.

Since the interaction of H₂O with oxygen over catalyst surface is inevitable in WGS reaction [28], the pre-adsorbed oxygen over catalyst surface significantly affects the adsorption and dissociation of H₂O [29,30], and the O–H bond cleavage [31–33]. Thus, the adsorption and dissociation of H₂O on the pre-adsorbed oxygen Cu(111) surface have also been investigated in experiment and theory. Salmeron et al. [34] used scanning tunneling microscopy (STM) to study the adsorption and reaction of H₂O molecule on Cu(110) surface partially covered with oxygen in the O(2×1) phase formed by Cu–O chains, suggesting that H₂O adsorbs at the edges and at the top of the Cu–O chains at 77 K, while H₂O reacts with O atoms in the chains to produce OH group at 155 K, the extent of H₂O dissociation is stoichiometrically determined by the amount of pre-adsorbed oxygen atoms. Theoretically, based on a $p(2 \times 2)$ Cu(111) model with the coverage of 0.25 ML using DFT method, Fang et al. [35,36] indicated that pre-adsorbed oxygen Cu(111) surface strengthens the interaction between H₂O and Cu surface, and weakens the interaction between OH and Cu surface, further promotes the catalytic activity of H₂O dissociation. Wang et al. [37] studied the adsorption and dissociation of a single H₂O on the clean and pre-adsorbed oxygen $p(3 \times 3)$ Cu(110) surface with the coverage of 0.11 ML using DFT calculations, indicating that compared to the clean surface, the pre-adsorbed oxygen surface can activate the H–O bond, and promote H₂O dissociation. Bu et al. [32] investigated the dissociation of a single H₂O on the clean and pre-adsorbed oxygen transition metal (Au, Ag, Cu, Pd, Rh, Ru, Ni) with a $p(3 \times 2)$ metal surface corresponding to the coverage of 0.17 ML, indicating that the stronger interaction between the oxygen atoms and the metal surface weakens the promoting effect on the O–H bond scission of H₂O. As mentioned above, these reported studies only focus on the single and low coverage of H₂O behavior on the clean and pre-adsorbed oxygen Cu surfaces, however, coverage-dependent H₂O adsorption and dissociation on the clean and pre-adsorbed oxygen Cu surface have not been well addressed, as a result, the coverage effect of H₂O on its adsorption and dissociation on Cu surface is still unclear.

On the other hand, it is well known that there are two kinds of interactions in H₂O/metal system; one is H₂O interaction with metal surface; the other is hydrogen-bond interaction among adsorbed H₂O molecules [38,39]. Based on DFT calculations, previous studies [40,41] calculated and compared the structure and electronic properties of the different adsorbed H₂O cluster on Cu(111) surface with that of the gas phase H₂O cluster to reveal the effect of metal surface on the adsorbed H₂O cluster and the binding nature between H₂O cluster and metal surface. Further, the isomers of adsorbed (H₂O)_n ($n = 1–6$) clusters on Cu(110) surface is studies, suggesting that the binding between H₂O and metal surface is greater than that between H₂O and H₂O molecule, which can be responsible for the relative stability of the isomers, and it is preference for more planar rather than buckled isomers. Above these theoretical studies only focus on understanding the reason and the role of Cu surface in H₂O cluster formation. However, as the number of H₂O molecule increases, the change trend of hydrogen-bond interaction between H₂O and H₂O molecule, as well as the interaction between H₂O cluster and metal surface still remain unclear. Therefore, the coverage effect of H₂O on the hydrogen-bond interaction and the interaction between H₂O cluster and metal surface needs to be illustrated at a molecular level.

In this study, the most stable Cu(111) surface is chosen to model Cu-catalyst, which is the dominant facet of WGS reaction in industrial catalytic reactions [43]. Here, we have systematically studied the adsorption of H₂O, HO, O, and H, as well as the dissociation of H₂O on the clean and pre-adsorbed oxygen Cu(111) surface. Meanwhile, we have also considered the effect of coverage on the adsorption and dissociation of H₂O using $p(1 \times 1)$, $p(2 \times 1)$, $p(2 \times 2)$ and $p(3 \times 3)$ Cu(111) surface models, which only consider the interaction between H₂O and metal surface. More importantly, except for the interaction between H₂O and metal surface, the hydrogen-bond interaction among adsorbed H₂O molecules play a key role in the formation of H₂O cluster [39]. Thus, as the number of H₂O molecule increases, the hydrogen-bond interaction among the adsorbed H₂O molecules, and the interaction between H₂O cluster and metal surface over Cu(111) surface have been also investigated.

2. Computational methods and models

2.1. Calculation method

All calculations have been performed using density functional theory (DFT) methods implemented in Dmol³ of Materials Studio 4.4 [44,45], where the exchange-correlation functional is described by the generalized gradient approximation (GGA) using Perdew–Burke–Ernzerhof (PBE) functional [46,47] together with the doubled numerical basis set plus polarization basis sets (DNP) [48]. The PBE functional has been widely used to investigate the reactions of small molecules on the metal surfaces, and the obtained results are often reliable [49,50]. Considering the weak interaction between H₂O and Cu surface, the adsorption and dissociation of H₂O molecule at 0.11 ML on the clean and pre-adsorbed oxygen Cu(111) surface using DFT-D2 correction method by Grimme [51] are calculated and compared. The related data are listed in Table S1 and the detailed descriptions are presented in the Part 1 of Supplementary material. The results show that H₂O prefers to desorption rather than its dissociation at 0.11 ML on the clean Cu(111) surface, while H₂O prefers to be dissociated rather than its desorption at 0.11 ML on the pre-adsorbed oxygen Cu(111) surface, which agree with the results without van der Waals correction. These results show that DFT-D2 correction method has few effects on our calculated results and qualitative conclusions. Previous studies [42,52] also showed that the consideration of vdW functional such as optPBE, optB88, revPBE does not alter the relative stabilities of structures predicted by PBE. In addition, although the total adsorption energies increase, the adsorption sites remain unchanged, and the adsorption geometries (water–metal bond and water H-bond lengths) are very similar between PBE and optB88-vdW functional [42]. Therefore, van der Waals forces have not been considered in this study. The inner electrons of Cu atom are kept frozen and replaced by an effective core potential (ECP) [53]; other atoms are treated with an all-electron basis set. A smearing of 0.005 Ha is applied to achieve accurate electronic convergence. Brillouin-zone integrations have been performed using $9 \times 9 \times 1$, $5 \times 9 \times 1$, $5 \times 5 \times 1$ and $3 \times 3 \times 1$ k-point grid for $p(1 \times 1)$, $p(2 \times 1)$, $p(2 \times 2)$ and $p(3 \times 3)$ surface, respectively. In addition, Mulliken charge analysis was calculated in our study, which can reveal that the interaction strength between adsorbates and substrate [54–56]. The fewer electrons transfer between adsorbates and substrate means the weaker interaction; whereas, the more electrons transfer between adsorbates and substrate means the stronger interaction.

In order to determine accurate activation barrier of the reaction, Complete LST/QST approach is used to search for transition states of the reactions [57]. Moreover, frequency analysis has been used to validate the transition state with only one imaginary frequency, and to obtain the zero-point energy; TS confirmation is performed on

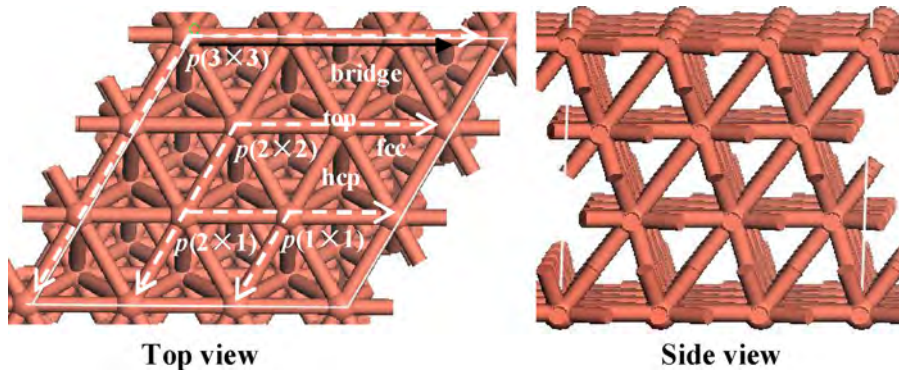


Fig. 1. Top and side views of the clean Cu(111)-(1×1), (2×1), (2×2) and (3×3) surfaces.

every transition state to confirm that it leads to the desired reactant and product.

For the elementary reaction such as $AB \rightarrow A + B$ on Cu(111) surface, the activation barrier (E_a) and reaction energy (ΔE) with zero-point energy (ZPE) correction refer to the following formulas:

$$E_a = E_{TS/Cu} - E_{AB/Cu} \quad (1)$$

$$\Delta E = E_{(A+B)/Cu} - E_{AB/Cu} \quad (2)$$

Where $E_{(A+B)/Cu}$ is the energy of the system with the co-adsorbed A and B species over Cu surface, $E_{AB/Cu}$ is the energy of AB species over Cu surface, $E_{TS/Cu}$ is the energy of transition state; these energies include ZPE correction.

2.2. Surface model

The face center cubic Cu unit cell was optimized, and the obtained lattice constant of 3.615 Å agrees well with the experimental data of 3.620 Å [58]. In this study, a periodic Cu(111) slab surface with four layers and a 10 Å vacuum layer is employed. The vacuum thickness is enough to separate the repeating slabs [59]. The different size of $p(1 \times 1)$, $p(2 \times 1)$, $p(2 \times 2)$ and $p(3 \times 3)$ surfaces are chosen to reflect the different coverage of 1.00, 0.50, 0.25 and 0.11 ML, respectively, this method has been widely used to investigate the different coverage of the adsorbates on metal surface to save the calculation cost [60–62], which is a simple, practicable and effective model. Ren *et al.* [24] and Hodgson *et al.* [63] have investigated the adsorption of $(H_2O)_6$ cluster on the $p(2 \times 2)$ Cu(110) and $p(2\sqrt{3} \times 2\sqrt{3})$ Ru(0001) surface. More importantly, similar to our study, Jiao *et al.* [64] study the adsorption for the different size of $(H_2O)_n$ ($n=2-6$) cluster over the $p(3 \times 4)$ Fe(100) surface. Further, the $p(3 \times 3)$ Cu(111) surface is used to model H_2O aggregation [24,63,64]. In order to mimic the real metal particles, the bottom one layer of Cu(111) slab surface is constrained at the bulk position, whereas the upper three layers together with the adsorbed species are allowed to relax. As shown in Fig. 1, there are four different adsorption sites on Cu(111) surface: Top, Bridge, Hcp, and Fcc.

3. Results and discussion

3.1. H, O and OH adsorption on Cu(111) surface at different coverage

The adsorption energy (E_{ads}) with zero-point energy (ZPE) correction is defined as follows:

$$E_{ads} = E_{adsorbate/Cu} - (E_{Cu} + E_{adsorbate}) \quad (3)$$

where E_{Cu} is the energy of the clean Cu slab, $E_{adsorbate}$ is the energy of free adsorbate, and $E_{adsorbate/Cu}$ is the energy for the system of Cu slab surface together with the adsorbed species; these energies include ZPE correction. With this definition, more negative values reflect the stronger interactions between the adsorbed species and Cu surface.

For OH adsorption, two adsorption modes, the O–H bond tilted from the surface and vertical to the surface, are considered. The most stable adsorption structures of H, O and OH species at different coverage within $p(3 \times 3)$, $p(2 \times 2)$, $p(2 \times 1)$ and $p(1 \times 1)$ Cu(111) surface are presented in Fig. 2. The adsorption energies (E_{ads}), the average bond lengths (d), and the electron transfer (q) between the adsorbed species and Cu surface at 0.11, 0.25, 0.50 and 1.00 ML are summarized in Table 1.

For H atom, the most stable adsorption sites are the hcp and fcc sites with the adsorption energies of -266.7 and $-266.8 \text{ kJ mol}^{-1}$ at 0.11 ML, -258.3 and $-259.2 \text{ kJ mol}^{-1}$ at 0.25 ML, -244.1 and $-244.9 \text{ kJ mol}^{-1}$ at 0.50 ML, and $-239.8 \text{ kJ mol}^{-1}$ at 1.00 ML, respectively, which agree in general with the previous studies by Jiang *et al.* [29,30] ($-247.5 \text{ kJ mol}^{-1}$ at the fcc site at 0.25 ML) and by Kandoi *et al.* [65] ($-246.0 \text{ kJ mol}^{-1}$ at the fcc site at 0.25 ML). Zu *et al.* [66] also experimentally confirmed that H atoms are adsorbed at three-fold hollow site on Cu(111) surface using the vibrational spectroscopy measurements. H atom adsorbed at the bridge site is less stable than that at the fcc or hcp site at 0.11 and 0.25 ML, while H atom adsorbed at the bridge site migrates to the fcc site as the coverage increases from 0.25 to 1.00 ML. The average distances between the adsorbed H and Cu atoms of three-fold hollow site agree well with the reported length of H–Cu bonds [67–71].

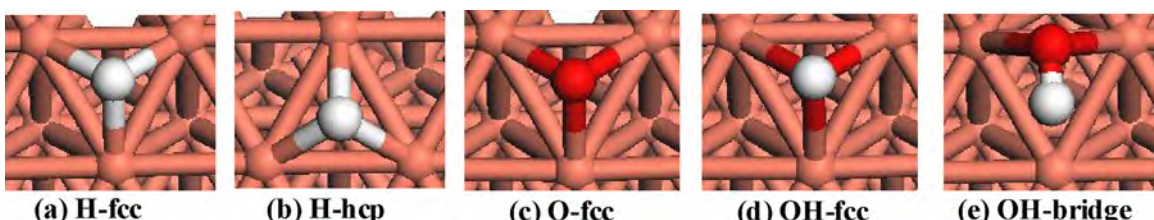


Fig. 2. The most stable configurations of OH, O and H species adsorbed on the clean Cu(111) surface.

Table 1

The adsorption energy (E_{ads} /kJ mol⁻¹), the average distance ($d/\text{\AA}$) from the adsorbate to Cu surface, and the charge transfer (q/e) to the adsorbates at the top, bridge, hcp and fcc sites at different coverage on the clean Cu(111) surface.

Adsorbate site	0.11 ML			0.25 ML			0.50 ML			1.00 ML		
	E_{ads}	d	q	E_{ads}	d	q	E_{ads}	d	q	E_{ads}	d	q
H-top	-208.7	1.518	0.035	-203.9	1.521	0.028				-156.0	1.505	0.120
H-bridge	-253.0	1.657	0.182	-245.8	1.656	0.179						
H-hcp	-266.7	1.737	0.228	-258.3	1.742	0.217	-244.1	1.729	0.244	-239.8	1.702	0.281
H-fcc	-266.8	1.736	0.234e	-259.2	1.741	0.220	-244.9	1.728	0.245	-239.8	1.702	0.279
O-top										-196.0	1.814	-0.108
O-hcp	-454.8	1.915	-0.476	-464.2	1.907	-0.462	-384.1	1.890	-0.352	-281.6	1.921	-0.178
O-fcc	-460.0	1.912	-0.472	-475.3	1.898	-0.457	-391.3	1.888	-0.350	-285.2	1.916	-0.177
OH-top	-253.3	1.879	-0.242				-172.7	1.855	-0.183	-197.4	1.891	-0.087
OH-bridge				-288.5	1.996	-0.250	-288.5	1.996	-0.250	-219.0	2.018	-0.126
OH-hcp	-301.0	2.059	-0.242	-302.3	2.070	-0.252						
OH-fcc	-304.5	2.053	-0.1696	-306.2	2.060	-0.245						

Milliken charge analysis indicates that electron transferred from H atom to Cu surface.

For O atom, it prefers to adsorb at the fcc site, as reported in the experimental and theoretical literatures [35,36,58,72–75], and the adsorption energies decrease with the increasing of coverage from 0.11 to 1.00 ML. The negative charge suggests that Cu acts as a donor, and O atom behaves as an electron acceptor. The small differences of charge transfer between fcc and hcp site agree with that of adsorption energy at different coverage.

For OH, it prefers to adsorb uprightly at the fcc sites via O atom, the adsorption energies are -304.5 and -306.2 kJ mol⁻¹ at 0.11 and 0.25 ML, respectively, which accords with the results of Phatak et al. at 0.11 ML [75] (-306.8 kJ mol⁻¹). When the coverage increases to 0.50 and 1.00 ML, OH prefers to adsorb at the bridge site rather than the fcc site with the adsorption energies of -288.5 and -219.0 kJ mol⁻¹, respectively. The O–H bond at the fcc site is perpendicular to the surface at 0.11 and 0.25 ML, while it is parallel to the surface at 0.50 and 1.00 ML. Charge transfer suggests that Cu surface acts as a donor, and OH behaves as an electron acceptor. There are no significant differences for adsorption site, adsorption energy, average distance and charge transfer obtained at 0.25 and 0.11 ML, respectively. However, it becomes different when the coverage increases from 0.25 to 1.00 ML, namely, OH adsorption on Cu catalyst is sensitive to the coverage.

Above results show that the adsorption site, adsorption energy, bond length, and electron transfer of H, O and OH species on Cu(111) surface are insensitive to the coverage from 0.11 to 0.25 ML. However, when the coverage increase from 0.25 to 1.00 ML, the adsorption energy, electron transfer of H, O and OH species at the most stable sites on Cu(111) surface decrease; and the corresponding bond lengths of Cu-X (H, O and OH) are also different. The most stable adsorption site of OH alters from three-fold hollow site to two-fold bridge site with the increasing of coverage. Further, the most favorable adsorption sites of OH, O, and H species are used to discuss H₂O dissociation on Cu(111) surface.

3.2. H₂O adsorption and dissociation on the clean Cu(111) surface at different coverage

3.2.1. H₂O adsorption

Four different adsorption orientations of H₂O at the four sites (top, bridge, fcc and hcp) have been investigated. As shown in Fig. 3, four different orientations in the initial structures are (a) H-up (H₂O molecular plane ($P_{\text{H}_2\text{O}}$) is normal to the substrate surface (P_{surf}) with two hydrogen atoms sitting at the same height, and two hydrogen atoms are above the oxygen atom), (b) H-down ($P_{\text{H}_2\text{O}}$ is normal to P_{surf} , with two hydrogen atoms sitting at the same height and below the oxygen atom), (c) H-down-up ($P_{\text{H}_2\text{O}}$ is normal to P_{surf} , with only one of O–H bonds pointing to the substrate surface), and (d) H-parallel ($P_{\text{H}_2\text{O}}$ is parallel to P_{surf}). Therefore, sixteen different initial adsorption configurations of H₂O molecule at four adsorption sites on Cu(111) surface were examined.

Fig. 4 presents the most stable adsorption configurations. The adsorption energies (E_{ads}), equilibrium distances (d) from H₂O molecule to the surface, and charge transfers (q) are listed in Table 2.

As shown in Table 2, H₂O molecule prefers to adsorb at the top site with the parallel mode, which have the adsorption energies of -54.4, -45.2, -46.3 and -20.3 kJ mol⁻¹ at the coverage of 0.11, 0.25, 0.50 and 1.00 ML, respectively. The adsorption site and configuration of H₂O accord with the results obtained by Michaelis's studies [17,39]. The equilibrium distances from the O atom of H₂O molecule to the nearest Cu atom are 2.454, 2.534, 2.838 and 3.479 Å, respectively. Meanwhile, as shown in Tables 1 and 2, compared to the electron transfer of about 0.25 e between the adsorbed H, O and OH species and Cu surface, there is small amount of electron transfer of 0.003 ~ 0.075 e between H₂O molecule and Cu surface, which reveals that H₂O molecule has a weaker interaction with Cu(111) surface compared to the adsorption of H, O and OH species. Thus, as the coverage increases from 0.11 to 1.00 ML, the adsorption energies of H₂O molecule decrease, and the distances between H₂O and substrate surface increase.

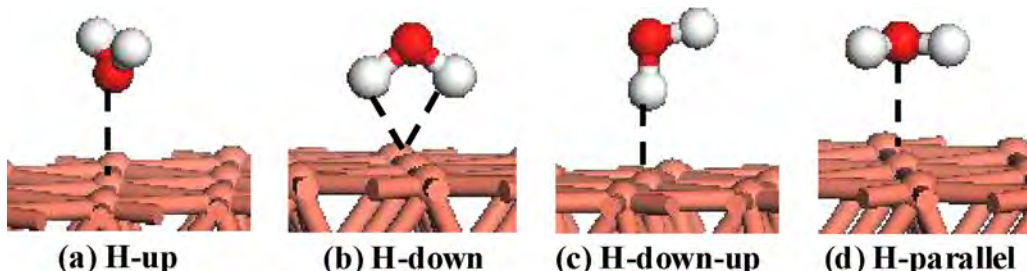


Fig. 3. H₂O molecule adsorbed at the top site with four different initial orientations on Cu(111) surface.

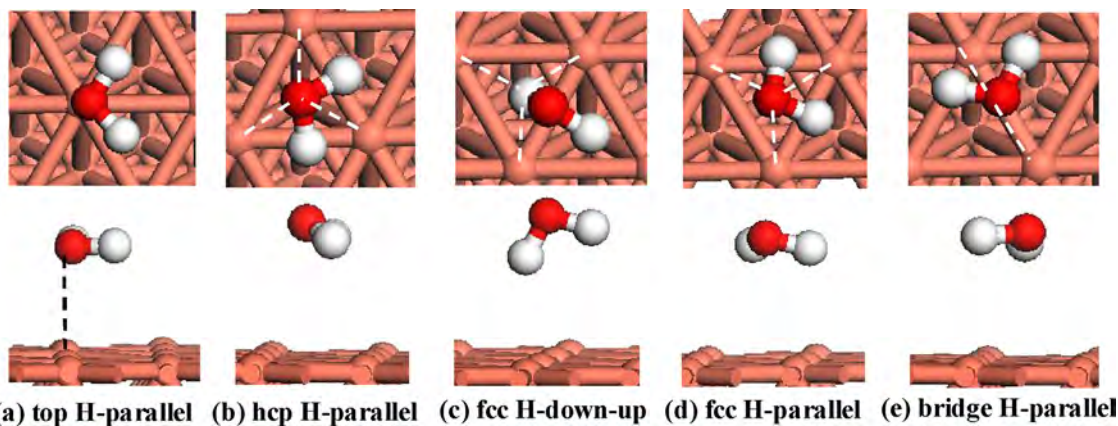


Fig. 4. The top and side views for the most stable configurations of H₂O molecule adsorbed at different site on Cu(111) surface.

Further, most of the initial structures with the different orientation are converted into the parallel model at different adsorption site at 0.50 and 1.00 ML (see Fig. S1). However, there are the modes of H-down-up or H-down with at least one O–H bonds pointing towards the surface except for the parallel model at 0.11 and 0.25 ML. These results indicate that there is the only parallel mode of H₂O molecule at the high coverage, while there are multi-model adsorptions of H₂O at the low coverage. Meanwhile, the H-parallel orientation is the most stable adsorption configuration among all different orientations.

3.2.2. H_2O dissociation

In this section, the complete dissociative processes of H_2O into $\text{O} + 2\text{H}$ via $\text{OH} + \text{H}$ have been investigated at the coverage of 0.11, 0.25, 0.50 and 1.00 ML based on the most stable adsorption structures of H_2O , OH , H and O species at the corresponding coverage. The potential energy of H_2O dissociation into O and 2H with the corresponding structures of initial state (IS), transition state (TS), and final state (FS) are shown in Figs. 5 and S2.

For H₂O dissociation into H and OH at 0.11, 0.25 and 0.50 ML, starting from H₂O adsorbed at the top site, it goes through the transition states (TS1-1, TS2-1 and TS3-1) to form OH and H species located at the adjacent fcc sites. In TS1-1, TS2-1 and TS3-1, the dissociating O-H distances are 1.640, 1.597 and 1.849 Å, and the forming Cu-H distances are 1.739, 1.760 and 1.660 Å, respectively. These reactions are endothermic by 22.4, 31.1 and 75.4 kJ mol⁻¹ with the activation barriers of 138.4, 129.9 and 141.8 kJ mol⁻¹ at 0.11, 0.25 and 0.50 ML, respectively. However, the adsorption energies are -54.4, -45.2 and -46.3 kJ mol⁻¹ at 0.11, 0.25 and 0.50 ML, respectively. Thus, H₂O molecule prefers to be desorption rather than being dissociated into OH+H at 0.11, 0.25 and 0.50 ML. Further, H₂O dissociation at 1.00 ML is considered, suggesting that when H and OH are initially adsorbed at the fcc and bridge sites, respectively, OH can easily interact with H atom to form H₂O molecule after geometry optimization. As a result,

H_2O dissociation is impossible at the higher coverage of 1.00 ML.

In addition, the transition state from the partial dissociated state (OH and H) to the fully dissociated products (2H and O) is examined (see Fig. S2). At 0.11 and 0.25 ML, in TS1-2 and TS2-2, H atoms are located at the top site with the $\text{Cu}-\text{H}$ distance of 1.578 and 1.649 Å, and the breaking $\text{O}-\text{H}$ distances are 1.743 and 1.633 Å, respectively; in the final state ($\text{O}+2\text{H}$), both O and H atoms are located at the fcc sites. The activation barriers and reaction energies are 168.6 and 67.7 kJ mol⁻¹ at 0.11 ML, 170.3 and 106.8 kJ mol⁻¹ at 0.25 ML, respectively. Further, the dissociation of OH and H into 2H and O at 0.50 ML suggests that when H and O are initially adsorbed at the adjacent fcc and hcp sites, H can easily interact with O to form OH after geometry optimization. Thus, the dissociation of OH with the co-adsorbed H is impossible at 0.50 ML.

The dissociation of the single OH radical into O and H at 0.11 and 0.25 ML was also considered (see Fig. S3), the dissociation needs the activation barriers of 163.6 and 154.8 kJ mol⁻¹, respectively. Both are endothermic by 67.9 and 87.3 kJ mol⁻¹, respectively. Compared to OH dissociation in the presence of hydrogen, the activation barriers of OH dissociation slightly decrease in the absence of hydrogen, namely, the co-adsorbed H atom on the surface is unfavorable for the dissociation of OH.

3.3. *H₂O adsorption and dissociation on pre-adsorbed oxygen Cu(111) surface at different coverage*

Pre-adsorbed oxygen over metal surface plays a key role in the O–H bond activation [37]. Thus, we probe into the adsorption and dissociation of H₂O on the pre-adsorbed oxygen Cu(111) surface. Considering that O atom prefers to adsorb at the fcc site, we choose the *p*(3 × 3), *p*(2 × 2), *p*(2 × 1) and *p*(1 × 1) Cu(111) surface with the adsorbed O atom at the fcc site as the pre-adsorbed oxygen surface models corresponding to the coverage of 0.11, 0.25, 0.50 and 1.00 ML, respectively.

Table 2

Table 2 The adsorption energy (E_{ads} /kJ mol $^{-1}$), average distance ($d/\text{\AA}$) from the O atom of H₂O to the adjacent Cu atom, and charge transfer (q/e) from H₂O to Cu surface for the most stable configurations of H₂O adsorbed at different site on Cu(111) surface.

Site orientation	0.11 ML			0.25 ML			0.50 ML			1.00 ML		
	E_{ads}	d	q									
top H-parallel	-54.4	2.454	0.075	-45.2	2.534	0.047	-46.3	2.838	0.025	-20.3	3.479	0.003
hcp H-parallel	-48.3	3.241	0.008	-39.5	3.218	0.010	-44.2	3.500	0.001	-19.8	3.896	0.001
fcc H-parallel				-39.5	3.228	0.010	-44.1	3.403	0.001	-19.8	3.873	0.001
fcc H-down-up	-47.4	2.776	0.019									
bridge H-parallel	-48.4	3.076	0.022	-39.8	3.158	0.009	-43.8	3.472	0.002	-19.9	3.841	0.001

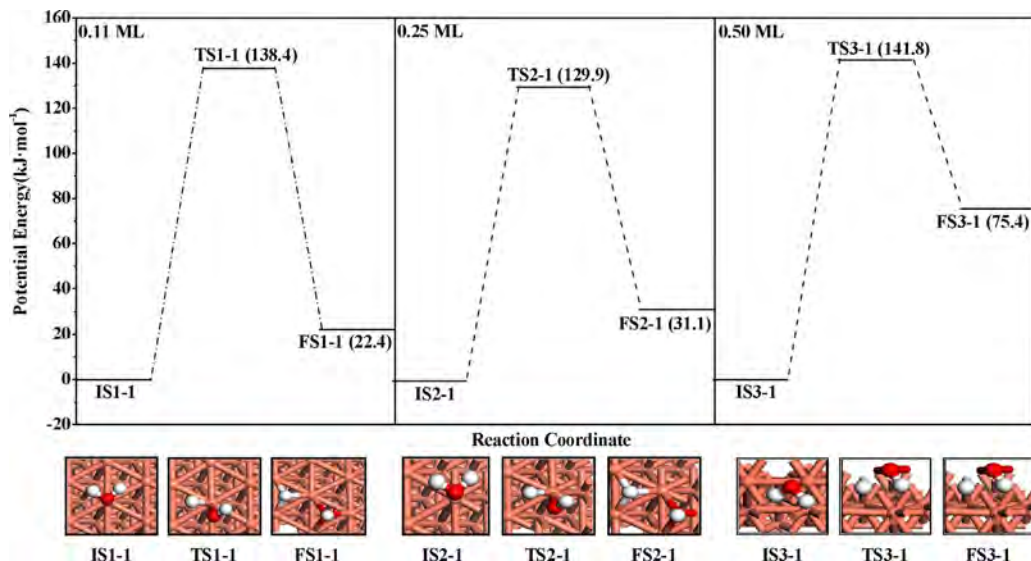


Fig. 5. The potential energy surfaces for H₂O dissociation into H + OH species on the clean Cu(111) surface at the coverage of 0.11, 0.25 and 0.50 ML, respectively. (IS1-1, 2-1, 3-1: the most stable adsorption state of H₂O molecule; TS1-1, 2-1, 3-1: the transition state; FS1-1, 2-1, 3-1: the final state of H atom and OH radical).

3.3.1. H₂O adsorption

For the adsorption of H₂O molecule on the pre-adsorbed oxygen Cu(111) surface, there are various co-adsorption structures between O at the fcc site and H₂O at the top, bridge, fcc and hcp site at the coverage of 0.11, 0.25, 0.50 and 1.00 ML, respectively, which have been examined in this section.

For the initial adsorption configurations of H₂O adsorption, as shown in Fig. 6, H_b atoms of H₂O molecule adsorbed nearby at the top site approach the pre-adsorbed oxygen atom (O_p) at the fcc site to form the hydrogen-bond between the H_b atom of H₂O and O_p atom with the distances of 1.942, 2.038 and 2.132 Å at 0.11, 0.25 and 0.50 ML, respectively. With the coverage increases, the O_w–H_b bond lengths become larger; the interaction between H₂O and the pre-adsorbed oxygen atom becomes weaker. Moreover, the O_w–H_b bond lengths (0.991, 0.986 and 0.997 Å for 0.11, 0.25 and 0.50 ML, respectively) of H₂O molecule are longer than those of H₂O adsorbed on Cu(111) surface and the gaseous H₂O (0.977 Å)

and 0.972 Å, respectively), suggesting that pre-adsorbed oxygen can largely activate the O–H bond of adsorbed H₂O. Meanwhile, the adsorption energies of H₂O on the pre-covered oxygen surface are –52.5, –58.6 and –50.7 kJ mol⁻¹ at 0.11, 0.25, and 0.50 ML, respectively. Although the coverage increases from 0.11 to 0.50 ML, the adsorption energies of H₂O change slightly. This reveals that pre-adsorbed oxygen reduces the coverage effect on H₂O adsorption at the coverage from 0.11 to 0.50 ML on the pre-adsorbed oxygen Cu(111) surface. In addition, the adsorption of H₂O molecule at 1.00 ML shows that H₂O becomes the dissociative adsorption to form two co-adsorbed OH species on the pre-adsorbed oxygen Cu(111) surface.

3.3.2. H₂O dissociation

Based on the most stable adsorption of H₂O on the pre-adsorbed oxygen Cu(111) surface, H₂O dissociation has been investigated at

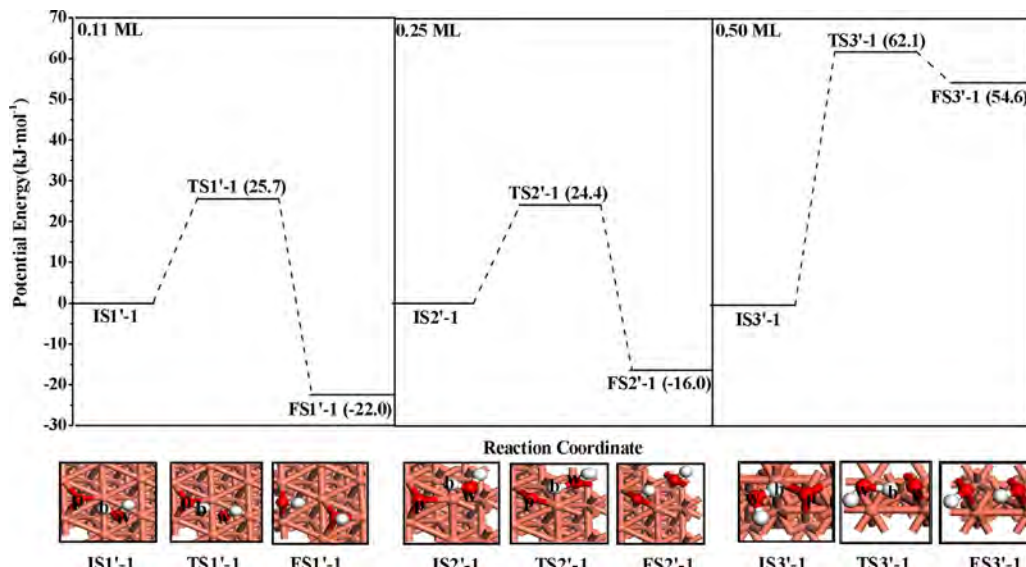


Fig. 6. The potential energy surfaces for H₂O dissociation into H + OH species on the pre-adsorbed oxygen Cu(111) surface at the coverage of 0.11, 0.25 and 0.50 ML, respectively. (IS1'-1, 2'-1, 3'-1: the most stable adsorption state of H₂O molecule; TS1'-1, 2'-1, 3'-1: the transition state; FS1'-1, 2'-1, 3'-1: the final state of 2OH radical; O_p and O_w denote the pre-adsorbed O atom and O atom of H₂O molecule, respectively; H_b denotes the nearest H atom of H₂O molecule with the pre-adsorbed O atom).

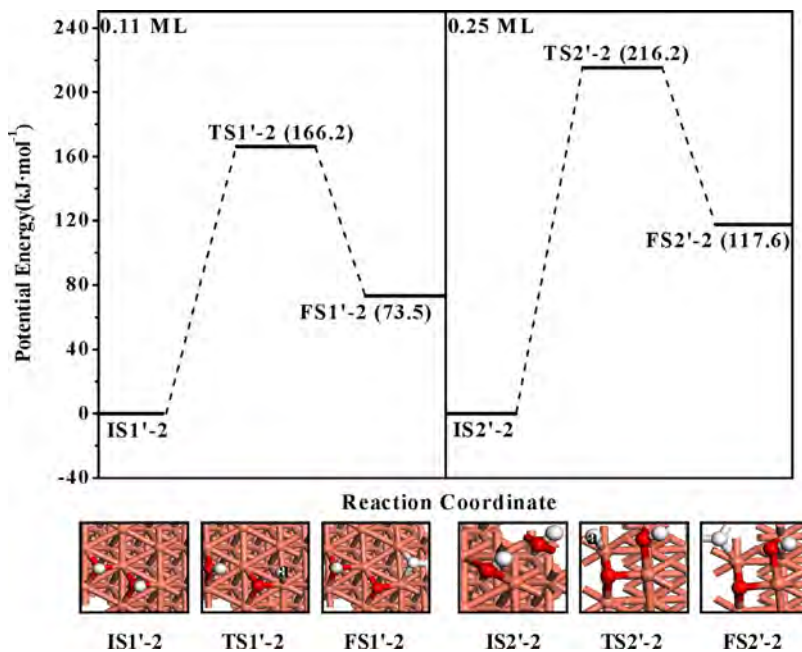


Fig. 7. The potential energy surfaces for $\text{H} + \text{OH}$ dissociation into $2\text{H} + \text{O}$ on the pre-adsorbed oxygen $\text{Cu}(111)$ surface at the coverage of 0.11 and 0.25 ML, respectively. ($\text{IS1}'\text{-}2$, $2'\text{-}2$: the most stable co-adsorption state of 2OH radical; $\text{TS1}'\text{-}2$, $2'\text{-}2$: the transition state; $\text{FS1}'\text{-}2$, $2'\text{-}2$: the final state of OH radical, O and H atom; H_a denotes the H atom of the dissociating OH radical).

0.11, 0.25 and 0.50 ML, respectively. As presented in Fig. 6, starting from the most adsorption configuration ($\text{IS1}'\text{-}1$, $2'\text{-}1$ and $3'\text{-}1$), the $\text{O}_\text{w}\text{-H}_\text{b}$ bond dissociates, and the departing H_b atom begins to coordinate with the pre-covered O_p atom to form hydroxyl $\text{O}_\text{p}\text{-H}_\text{b}$ in the final state ($\text{FS1}'\text{-}1$, $2'\text{-}1$ and $3'\text{-}1$). The cleavage of $\text{O}_\text{w}\text{-H}_\text{b}$ bond goes through the transition state ($\text{TS1}'\text{-}1$, $2'\text{-}1$ and $3'\text{-}1$) with the activation barrier of 25.7, 24.4 and 62.1 kJ mol^{-1} , and the process are exothermic by 22.0, 16.0 at 0.11 and 0.25 ML and endothermic by 54.6 kJ mol^{-1} at 0.50 ML, respectively. The distances of dissociating $\text{O}_\text{w}\text{-H}_\text{b}$ and forming $\text{O}_\text{p}\text{-H}_\text{b}$ bonds are 0.962 and 1.164 Å in $\text{TS1}'\text{-}1$ at 0.11 ML, and 1.123 and 1.438 Å in $\text{TS2}'\text{-}1$ at 0.25 ML, and 1.239 and 1.224 Å in $\text{TS3}'\text{-}1$ at 0.50 ML. In the final state, two OH adsorb at the bridge and fcc sites at 0.11 ML respectively, while both prefer to adsorb at two adjacent bridge sites at 0.25 and 0.50 ML.

Compared to H_2O desorption, H_2O prefers to dissociate into two OH at 0.11 and 0.25 ML. However, H_2O prefers to be desorption rather than its dissociation at 0.50 ML due to high dissociation barrier. Thus, compared to the clean surface, the pre-adsorbed oxygen significantly facilitates H_2O dissociation to form two adsorbed OH species at the coverage below 0.50 ML.

Further, starting from two adsorbed OH species, H atom can further be removed from OH fragment to form H and O atoms, in which we only consider the dissociation of $\text{O}_\text{w}\text{-H}_\text{a}$ on the surface, as presented in Fig. 7. This step goes through H_a atom migration from O_w atom to the fcc site to form OH , O and H species, and this reaction is highly endothermic by 73.5 and 117.6 kJ mol^{-1} with the activation barriers of 166.2 and 216.2 kJ mol^{-1} at 0.11 and 0.25 ML, respectively. Correspondingly, the distances of dissociating $\text{O}_\text{w}\text{-H}_\text{b}$ bond are 1.669 and 1.642 Å, respectively. However, the dissociation of the co-adsorbed $\text{OH} + \text{OH}$ species into the co-adsorbed $\text{O} + \text{H} + \text{OH}$ species is impossible at 0.50 ML. The reason is that when O and H atoms are initially placed at the fcc sites in the final state, O and H atoms can again interact to form OH after geometry optimization. Namely, there is no available adsorption site for OH dissociation at 0.50 ML.

Therefore, for H_2O dissociation into 2OH , followed by the $\text{O}\text{-H}$ bond cleavage to form the co-adsorbed OH , O and H species at the

coverage below 0.50 ML, the dissociation barrier increases with the increasing of coverage; H_2O prefers to be dissociated into OH compared to its desorption from the surface, however, OH further dissociates into O and H atoms cannot occur. When the coverage is above 0.50 ML, H_2O prefers to desorption rather than its dissociation. Therefore, H_2O dissociation on the pre-adsorbed oxygen $\text{Cu}(111)$ surface depends on the coverage and pre-adsorbed oxygen.

3.4. H_2O aggregation on $\text{Cu}(111)$ surface

For H_2O aggregation on $\text{Cu}(111)$ surface, the formation energy (E_{form}) of $(\text{H}_2\text{O})_n$ cluster on $\text{Cu}(111)$ surface involves two kinds of interactions; one is hydrogen-bond interaction (E_H) among adsorbed $(\text{H}_2\text{O})_n$ molecules; the other is the interaction between $(\text{H}_2\text{O})_n$ cluster and metal surface, which is defined as the adsorption energy (E_{ads}^c) of $(\text{H}_2\text{O})_n$ cluster. Here, the formation energy (E_{form}) of $(\text{H}_2\text{O})_n$ cluster is defined as follows:

$$E_{\text{form}} = [E_{(\text{H}_2\text{O})_n/\text{Cu}} - (E_{\text{Cu}} + nE_{\text{H}_2\text{O}})]/n \quad (4)$$

Where n is the number of H_2O molecule in $(\text{H}_2\text{O})_n$ cluster, E_{Cu} is the energy of the clean Cu slab surface, $E_{\text{H}_2\text{O}}$ is the energy of H_2O molecule, and $E_{(\text{H}_2\text{O})_n/\text{Cu}}$ is the energy for the system of Cu slab surface together with the adsorbed $(\text{H}_2\text{O})_n$ cluster. With this definition, more negative values of E_{form} reflect that the formation of $(\text{H}_2\text{O})_n$ cluster becomes more easier on Cu surface. Based on the optimized structure of adsorbed $(\text{H}_2\text{O})_n$ cluster on Cu surface, the single point energy of $(\text{H}_2\text{O})_n$ cluster alone is calculated. Then, the hydrogen-bond interaction (E_H) and adsorption energy (E_{ads}^c) of $(\text{H}_2\text{O})_n$ are obtained as follows:

$$E_\text{H} = (E_{(\text{H}_2\text{O})_n} - nE_{\text{H}_2\text{O}})/n \quad (5)$$

$$E_{\text{ads}}^c = E_{\text{form}} - E_\text{H} \quad (6)$$

Where $E_{(\text{H}_2\text{O})_n}$ is the single point energy of $(\text{H}_2\text{O})_n$ cluster; these energies include ZPE correction. The more negative values of E_H and E_{ads}^c reflect the stronger hydrogen-bond interaction among $(\text{H}_2\text{O})_n$ cluster, and the stronger interaction of $(\text{H}_2\text{O})_n$ cluster with Cu surface, respectively.

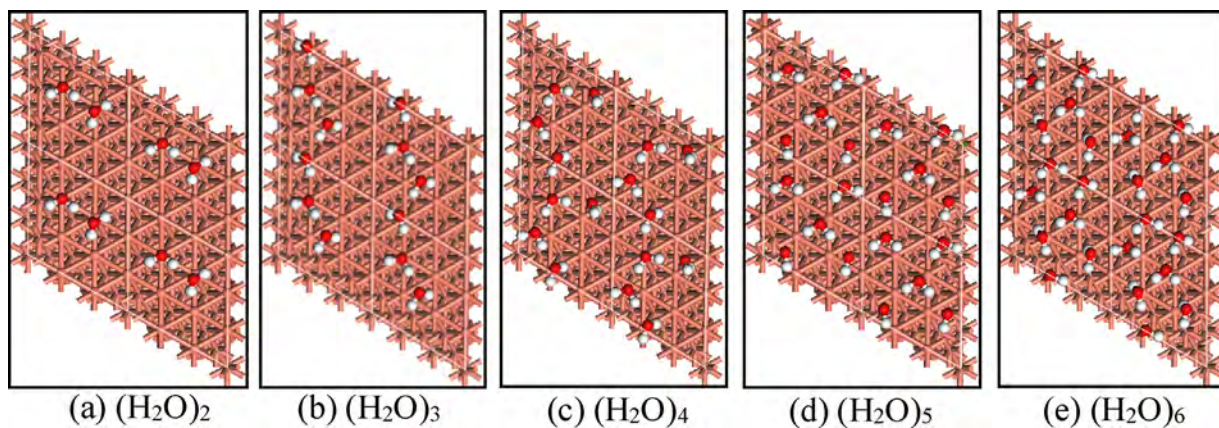


Fig. 8. The most stable adsorption configurations of H_2O aggregation at different coverage on $\text{Cu}(111)$ surface.

As mentioned above, when the interaction of H_2O with Cu surface is considered, it is noted that H_2O adsorption on $\text{Cu}(111)$ surface at higher coverage, two kinds of interactions between H_2O and metal surface exist, one is H_2O interacting with metal surface; the other is the hydrogen-bond interaction among the adsorbed H_2O molecules, which can facilitate the formation of $(\text{H}_2\text{O})_n$ cluster on Cu surface, thus, it is necessary to investigate H_2O aggregation over $\text{Cu}(111)$ surface in order to understand H_2O interaction with Cu surface and the hydrogen-bond interaction among the adsorbed H_2O molecules.

The interaction of H_2O clusters within a $p(3 \times 3)$ $\text{Cu}(111)$ surface was modeled (see Fig. 8) in this section. The initial structures of $(\text{H}_2\text{O})_n$ on $\text{Cu}(111)$ surface were estimated according to the most stable position of a single H_2O molecule adsorbed on the surface at equilibrium. The formation energy, hydrogen-bond interaction and the adsorption energy of $(\text{H}_2\text{O})_n$ cluster over $\text{Cu}(111)$ surface are presented in Table 3.

For $n=2$, the dimer cluster exhibits the “discontinuous linear” shape with the formation energy of $-61.1 \text{ kJ mol}^{-1}$. The adsorption energy is $-50.1 \text{ kJ mol}^{-1}$, which is similar to that of the single H_2O molecule. As shown in Fig. 8a, one H_2O molecule is adsorbed at the top site with the $\text{Cu}-\text{O}$ distance of 2.229 \AA , which is shorter than that of single H_2O adsorption (2.454 \AA). The O atom of the second H_2O molecule forms the hydrogen-bond interaction with one H atom of the first adsorbed H_2O molecule, the hydrogen-bond interaction is $-11.0 \text{ kJ mol}^{-1}$, and the corresponding $\text{H}-\text{O}$ distance

Table 3

The formation energy ($E_{\text{form}}/\text{kJ mol}^{-1}$), adsorption energy ($E_{\text{ads}}^{\text{c}}/\text{kJ mol}^{-1}$) and hydrogen-bond interaction energy ($E_{\text{H}}/\text{kJ mol}^{-1}$), charge transfer (q and \bar{q}/e) for $(\text{H}_2\text{O})_n$ on $\text{Cu}(111)$ surface.

$(\text{H}_2\text{O})_n$	$E_{\text{form}}/\text{kJ mol}^{-1}$	$E_{\text{ads}}^{\text{c}}/\text{kJ mol}^{-1}$	$E_{\text{H}}/\text{kJ mol}^{-1}$	q/e	\bar{q}/e
1	-54.4	-54.4	0.0	0.075	0.075
2	-61.1	-50.1	-11.0	0.116	0.058
3	-65.1	-33.0	-32.1	0.088	0.029
4	-65.4	-30.1	-35.3	0.113	0.028
5	-64.9	-20.3	-44.6	0.006	0.001
6	-67.5	-22.6	-44.9	0.129	0.022

is 1.750 \AA . Two H atoms of the second H_2O molecule point to Cu surface without hydrogen-bond interaction.

For $n=3$, the trimer cluster forms the “continuous linear” shape releasing the energy of 65.1 kJ mol^{-1} . The adsorption energy is $-33.0 \text{ kJ mol}^{-1}$. As shown in Fig. 8b, the middle H_2O molecule can form the hydrogen-bond interaction with the adjacent H_2O molecule by providing the H atom with a hydrogen-bond distance of 1.701 \AA , and with another H_2O molecule by accepting H atom with hydrogen-bond distance of 1.825 \AA . The corresponding average hydrogen-bond interaction is $-32.1 \text{ kJ mol}^{-1}$.

Similar to $(\text{H}_2\text{O})_3$ cluster, the formation and adsorption energy for the semi-ring shape of $(\text{H}_2\text{O})_4$ cluster are -65.4 and $-30.1 \text{ kJ mol}^{-1}$, respectively. There are four hydrogen-bonds among four H_2O molecules with the distances of 1.893 , 1.751 ,

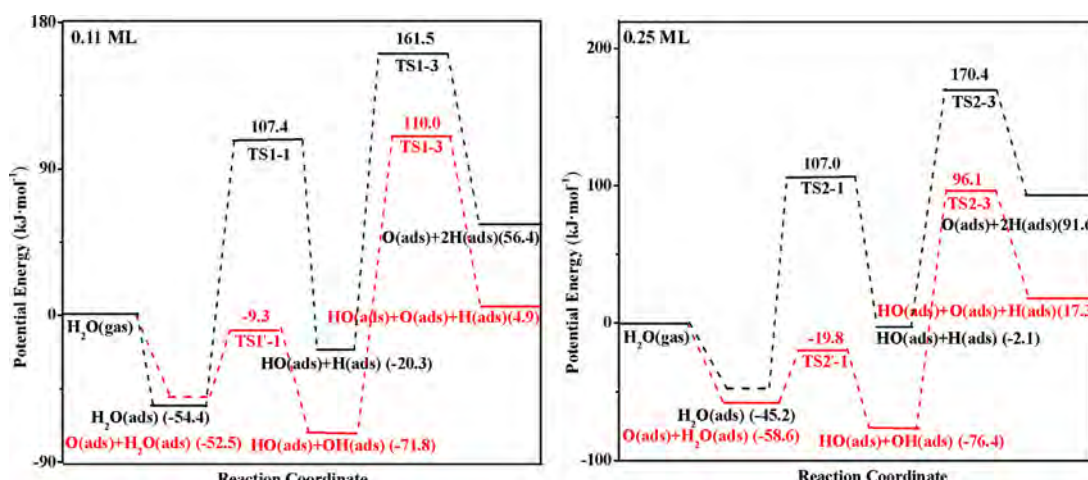


Fig. 9. The potential energy surfaces for the complete dissociation of H_2O molecule at the coverage of 0.11 and 0.25 ML , respectively. Black line: the clean $\text{Cu}(111)$ surface; Red line: the pre-adsorbed oxygen $\text{Cu}(111)$ surface. (For interpretation of the references to colour in this figure legend, the reader is referred to the web version of this article.)

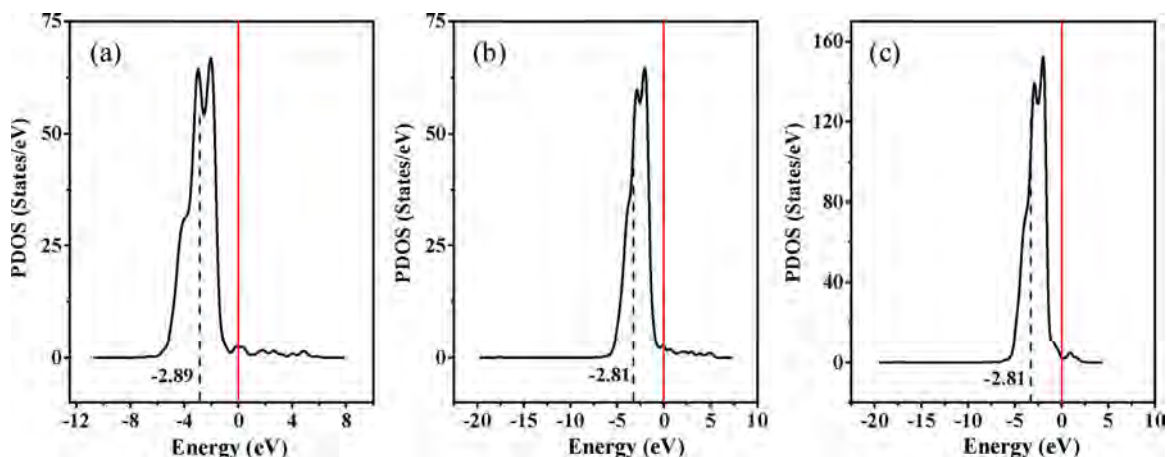


Fig. 10. Projected density of states plots for the *d*-band of (a) the clean Cu(111) surface, (b) the pre-adsorbed oxygen *p*(2 × 2) Cu(111) surface, (c) the pre-adsorbed oxygen *p*(2 × 3) Cu(111) surface. The dotted line denotes the position of *d*-band center. Red line at 0 eV denotes Fermi level. (For interpretation of the references to colour in this figure legend, the reader is referred to the web version of this article.)

1.857 and 2.057 Å, respectively. The corresponding hydrogen-bond interaction is $-35.3 \text{ kJ mol}^{-1}$. Compared to $(\text{H}_2\text{O})_2$ cluster, the adsorption energy of $(\text{H}_2\text{O})_{3,4}$ cluster decreases by 20.0 kJ mol^{-1} , while the hydrogen-bond interaction increases by 20.0 kJ mol^{-1} .

For $n=5$, five H_2O molecules can form the ring shape with the energy of $-64.9 \text{ kJ mol}^{-1}$. There are five hydrogen-bonds with the distances of 1.803, 1.876, 1.988, 1.853 and 2.100 Å, respectively. The average hydrogen-bond interaction and the adsorption energy are -44.6 and $-20.3 \text{ kJ mol}^{-1}$, respectively.

For $n=6$, six H_2O molecules can form a five-membered ring with one exocyclic H_2O molecule. There are six hydrogen-bonds with the distances of 1.763, 1.857, 1.711, 1.852, 2.376 and 2.444 Å, respectively. The average hydrogen-bond interaction and the adsorption energy of $(\text{H}_2\text{O})_6$ cluster are -44.9 and $-22.6 \text{ kJ mol}^{-1}$, respectively. Compared to $(\text{H}_2\text{O})_{3,4}$ cluster, the adsorption energy of $(\text{H}_2\text{O})_{5,6}$ cluster decreases by 10.0 kJ mol^{-1} , the hydrogen-bond interaction of $(\text{H}_2\text{O})_{5,6}$ cluster increases by 10.0 kJ mol^{-1} .

Above results show that as the number of aggregate H_2O molecules increases, the formation energy of $(\text{H}_2\text{O})_n$ cluster becomes more negative, namely, H_2O aggregation becomes easier on Cu surface. Moreover, the adsorption energy decreases with the increasing number of H_2O molecule, the small amount of transferred charge in the range of $0.001 \sim 0.058 \text{ eV}$ indicate the weak interaction between $(\text{H}_2\text{O})_n$ cluster and Cu(111) surface.

3.5. General discussion

For H_2O adsorption, compared to the clean surface, there are almost similar adsorption structures and energies of H_2O molecule on the pre-adsorbed oxygen Cu(111) with the increases of coverage, indicating that the coverage has no effect on H_2O adsorption over the pre-adsorbed oxygen Cu(111) surface. However, for H_2O dissociation, as shown in Fig. 9, compared to the clean surface, the pre-adsorbed oxygen atom reduces significantly the activation barrier of H_2O dissociation, such as the difference of $118.6 \text{ kJ mol}^{-1}$ for 0.11 ML and $113.4 \text{ kJ mol}^{-1}$ for 0.25 ML; and changes from endothermic reaction to exothermic one. The results show that the hydroxyl groups are formed more easily on the pre-adsorbed oxygen surface. The formed hydroxyl groups can hardly undergo further dissociation due to higher barrier, namely, the formed OH group from H_2O dissociation is stable on Cu(111).

When the coverage increases to 0.50 ML, H_2O molecule prefers to desorb from Cu surface rather than being dissociated into OH

and H regardless of the presence or absence of pre-adsorbed oxygen on Cu(111) surface. Thus, for the coverage below 0.50 ML, the pre-adsorbed oxygen promotes the production of OH group, and accelerates the hydroxylation rate of Cu(111) surface, but not for the coverage above 0.50 ML.

In order to understand the underlying electronic properties, the effect of pre-adsorbed oxygen on the electronic structure of Cu(111) surface is investigated in terms of *d*-band center. Fig. 10 shows the calculated PDOS plot for the *d*-band of the clean and pre-adsorbed oxygen Cu(111) surfaces, the *d*-band center (dash line) can reflect the catalytic activity of Cu catalyst toward H_2O dissociation. It is found that compared to the clean surface (see Fig. 10a), there are the negligible downshifts of *d*-band centers for pre-adsorbed oxygen Cu surface (see Fig. 10b and c), and there are the equivalent values of *d*-band center at different coverage of 0.11 and 0.25 ML, respectively. This analysis clearly demonstrates that the oxygen-modified Cu surface doesn't or weakly alters the *d*-band centers of surface Cu atoms. On the other hand, the formed hydrogen-bonds between the adsorbed O atom and H atom of H_2O molecule play a key role in the O–H bond cleavage of H_2O molecule. Therefore, to some extent, it can be concluded that the amount of the adsorbed oxygen atoms directly determines the rate of H_2O dissociation, and further determines the activity of WGS reaction on the oxygen-modified Cu surface.

For H_2O aggregates on Cu(111) surface, as listed in Table 3, the adsorption energies of monomer and dimer with one hydrogen-bond are about $-50.0 \text{ kJ mol}^{-1}$; the trimer and tetramer show the lower adsorption energy of about $-30.0 \text{ kJ mol}^{-1}$; as for the pentamer and hexamer, the adsorption energy reduces to about $-20.0 \text{ kJ mol}^{-1}$. As the number of H_2O molecules increases in the aggregation, the adsorption energy of $(\text{H}_2\text{O})_n$ cluster over Cu(111) surface decreases, indicating that the interaction between $(\text{H}_2\text{O})_n$ and Cu surface becomes weaker with the increasing number of H_2O molecules. On the other hand, as shown in Fig. 8 and Table 3, there is no hydrogen-bond and only one hydrogen-bond with the hydrogen-bond energy of $-11.1 \text{ kJ mol}^{-1}$ for the monomer and dimer; three hydrogen-bonds in the trimer and four hydrogen-bonds in the tetramer with the hydrogen-bond energy of about $-30.0 \text{ kJ mol}^{-1}$; five hydrogen-bonds in the pentamer and six hydrogen-bonds in the hexamer with the hydrogen-bond energy of about $-45.0 \text{ kJ mol}^{-1}$. It is concluded that the interaction of hydrogen-bond among $(\text{H}_2\text{O})_n$ cluster becomes stronger with the increasing number of H_2O molecules.

4. Conclusions

In this study, we have investigated the adsorption and dissociation of H₂O on the clean and pre-adsorbed oxygen Cu(111) surfaces at different coverage, as well as H₂O aggregation on Cu(111) surface using DFT calculations. For H, O and OH species, as the coverage increases, the interaction between adsorbed species and Cu surface becomes weaker.

For H₂O molecule adsorption on the clean Cu(111) surface, as the coverage increases, the adsorption energy decreases, the distance between H₂O and substrate surface increases, and the orientation of H₂O adsorption is different, namely, only the parallel adsorption mode of H₂O molecule exists at high coverage while multi-model adsorptions of H₂O at low coverage on the clean surface. Meanwhile, the H-parallel orientation is the most stable adsorption configuration at different coverage. However, compared to the clean surface, the pre-adsorbed oxygen reduces the effect of coverage on H₂O adsorption at the coverage from 0.11 to 0.50 ML on the pre-adsorbed oxygen surface.

Further, H₂O dissociation becomes more difficult on both the clean and pre-adsorbed oxygen Cu(111) surface as the coverage increases. However, H₂O molecule will dissociate into OH instead of its desorption on the pre-adsorbed oxygen Cu(111) surface until the coverage reaches 0.50 ML, whereas H₂O molecule prefers to desorb rather than being dissociated on the clean Cu(111) surface at different coverage. Thus, the dissociation of H₂O depends on the coverage and pre-adsorbed oxygen. Compared to the clean surface, the oxygen reduces significantly the activation barrier of H₂O dissociation into OH on the pre-adsorbed oxygen surface, while OH further dissociation into O and H is difficult. Thus, to some extent, the amount of adsorbed oxygen atoms on Cu catalyst surface directly determines the rate of H₂O dissociation, further determines the catalytic activity of WGS reaction on the oxygen-modified Cu surface.

On the other hand, for H₂O aggregation on Cu(111) surface, as the number of H₂O molecule increases, the aggregation becomes easier due to the increasing interaction of hydrogen-bond among adsorbed H₂O molecules; whereas the interaction between (H₂O)_n and Cu surface becomes weaker.

Acknowledgments

This work is financially supported by the National Natural Science Foundation of China (No. 21476155, 21736007 and 21776193), the China Scholarship Council (201606935026), the Program for the Top Young Academic Leaders of Higher Learning Institutions of Shanxi, the Top Young Innovative Talents of Shanxi.

Appendix A. Supplementary data

Supplementary data associated with this article can be found, in the online version, at <http://dx.doi.org/10.1016/j.mcat.2017.11.034>.

References

- [1] I. Chorkendorff, J.W. Niemantsverdriet, *Concepts of Modern Catalysis and Kinetics*, Wiley-VCH, Weinheim, Germany, 2005.
- [2] C.V. Ovesen, P. Stoltze, J.K. Nørskov, C.T. Campbell, A kinetic model of the water gas shift reaction, *J. Catal.* 134 (1992) 445–468.
- [3] C.V. Ovesen, B.S. Clausen, B.S. Hammershøi, G. Steffensen, T. Askgaard, I. Chorkendorff, J.K. Nørskov, P.B. Rasmussen, P. Stoltze, P. Taylor, A microkinetic analysis of the water-gas shift reaction under industrial conditions, *J. Catal.* 158 (1996) 170–180.
- [4] D.J. Dwyer, F.M. Hoffmann, *Surface Science of Catalysis: In Situ Probes and Reaction Kinetics*, American Chemical Society, Washington, 1992.
- [5] Q. Fu, H. Salzburg, M. Flytzani-Stephanopoulos, Active nonmetallic Au and Pt species on ceria-based water-gas shift catalysts, *Science* 301 (2003) 935–938.
- [6] J.A. Rodriguez, P. Liu, J. Hrbek, J. Evans, M. Pérez, Water gas shift reaction on Cu and Au nanoparticles supported on CeO₂(111) and ZnO: intrinsic activity and importance of support interactions, *Angew. Chem. Int. Ed.* 46 (2007) 1329–1332.
- [7] T.S. Askgaard, J.K. Nørskov, C.V. Ovesen, P. Stoltze, A kinetic model of methanol synthesis, *J. Catal.* 156 (1995) 229–242.
- [8] A.Y. Rozovskii, C.I. Lin, Fundamentals of methanol synthesis and decomposition, *Top. Catal.* 22 (2003) 137–150.
- [9] J.A. Rodríguez, J. Evans, J. Graciani, J.B. Park, P. Liu, J. Hrbek, J.F. Sanz, High water-gas shift activity in TiO₂(110) supported Cu and Au nanoparticles: role of the oxide and metal particle size, *J. Phys. Chem. C* 113 (2009) 7364–7370.
- [10] J.A. Rodriguez, J. Graciani, J. Evans, J. B. Park, F. Yang, D. Stacchiola, S.D. Senanayake, S.G. Ma, M. Pérez, P. Liu, F.J. Sanz, J. Hrbek, Water-gas shift reaction on a highly active inverse CeO_x/Cu(111) catalyst: unique role of ceria nanoparticles, *Angew. Chem. Int. Ed.* 48 (2009) 8047–8050.
- [11] P.A. Thiel, T.E. Maday, The interaction of water with solid surfaces: fundamental aspects, *Surf. Sci. Rep.* 7 (1987) 211–385.
- [12] M.A. Henderson, The interaction of water with solid surfaces: fundamental aspects revisited, *Surf. Sci. Rep.* 46 (2002) 1–308.
- [13] A. Verdaguera, G.M. Sacha, H. Bluhm, M. Salmeron, Molecular structure of water at interfaces: wetting at the nanometer scale, *Chem. Rev.* 106 (2006) 1478–1510.
- [14] A. Hodgson, S. Haq, Water adsorption and the wetting of metal surfaces, *Surf. Sci. Rep.* 64 (2009) 381–451.
- [15] P. Feibelman, The first wetting layer on a solid, *Phys. Today* 63 (2010) 34–39.
- [16] J. Carrasco', A. Hodgson, A. Michaelides, A molecular perspective of water at metal interfaces, *Nat. Mater.* 11 (2012) 667–674.
- [17] A. Michaelides, V.A. Ranea, P.L. de Andres, D.A. King, General model for water monomer adsorption on close-packed transition and noble metal surfaces, *Phys. Rev. Lett.* 90 (2003), 216102-1–4.
- [18] C.T. Au, J. Breza, M.W. Roberts, Hydroxylation and dehydroxylation at Cu(111) surfaces, *Chem. Phys. Lett.* 66 (1979) 340–343.
- [19] J. Nakamura, J.M. Campbell, C.T. Campbell, Kinetics and mechanism of the water-gas shift reaction catalysed by the clean and Cs-promoted Cu(110) surface: a comparison with Cu(111), *J. Chem. Soc. Faraday Trans.* 86 (1990) 2725–2734.
- [20] J. Kubota, J. Kondo, K. Domen, C. Hirose, An IRAS study of hydroxyl species (OD(a)) on oxygen-modified Cu(110) surface, *Surf. Sci.* 295 (1993) 169–173.
- [21] K. Prabhakaran, P. Sen, C.N.R. Rao, Hydroxylation of oxygen-covered Cu(110) and Zn(0001) surfaces by interaction with CH₃OH, (CH₃)₂NH, H₂S, HCl and other proton donor molecules, *Surf. Sci.* 169 (1986) L301–L306.
- [22] C.D. Taylor, Atomistic modeling of corrosion events at the interface between a metal and its environment, *Int. J. Corros.* 2012 (2012) 1–13.
- [23] Q.L. Tang, Z.X. Chen, Density functional slab model studies of water adsorption on flat and stepped Cu surfaces, *Surf. Sci.* 601 (2007) 954–964.
- [24] J. Ren, S. Meng, Atomic structure and bonding of water overlayer on Cu(110): the borderline for intact and dissociative adsorption, *J. Am. Chem. Soc.* 128 (2006) 9282–9283.
- [25] P. Zhang, W.T. Zheng, Q. Jiang, Behaviors of monomer H₂O on the Cu(111) surface under surface charges, *J. Phys. Chem. C* 114 (2010) 19331–19337.
- [26] J.L.C. Fajin, M.N.D.S. Cordeiro, F. Illas, J.R.B. Gomes, Influence of step sites in the molecular mechanism of the water gas shift reaction catalyzed by copper, *J. Catal.* 268 (2009) 131–141.
- [27] H. Ruuska, T.A. Pakkanen, R.L. Rowley, MP2 study on water adsorption on cluster models of Cu(111), *J. Phys. Chem. B* 108 (2004) 2614–2619.
- [28] K. Bange, D.E. Grider, T.E. Maday, J.K. Sass, The surface chemistry of H₂O on clean and oxygen-covered Cu(110), *Surf. Sci.* 136 (1984) 38–64.
- [29] M. Wolf, S. Nettesheim, J.M. White, E. Hasselbrink, G. Ertl, Ultraviolet-laser induced dissociation and desorption of water adsorbed on Pd(111), *J. Chem. Phys.* 92 (1990) 1509–1510.
- [30] M. Wolf, S. Nettesheim, J.M. White, E. Hasselbrink, G. Ertl, Dynamics of the ultraviolet photochemistry of water adsorbed on Pd(111), *J. Chem. Phys.* 94 (1991) 4609–4619.
- [31] L. Jiang, G.C. Wang, Z.S. Cai, Y.M. Pan, X.Z. Zhao, Promotion of the water-gas shift reaction by pre-adsorbed oxygen on Cu(hkl) surfaces: a theoretical study, *J. Mol. Struc.: Theochim.* 710 (2004) 97–104.
- [32] G.C. Wang, S.X. Tao, X.H. Bu, A systematic theoretical study of water dissociation on clean and oxygen-preadsorbed transition metals, *J. Catal.* 244 (2006) 10–16.
- [33] Y.Q. Wang, L.F. Yan, G.C. Wang, Oxygen-assisted water partial dissociation on copper: a model study, *Phys. Chem. Chem. Phys.* 17 (2015) 8231–8238.
- [34] Z. Pang, S. Duerrbeck, C. Kha, E. Bertel, G.A. Somorjai, M. Salmeron, Adsorption and reactions of water on oxygen-precovered Cu(110), *J. Phys. Chem. C* 120 (2016) 9218–9222.
- [35] Z. Jiang, T. Fang, Dissociation mechanism of H₂O on clean and oxygen-covered Cu(111) surfaces: a theoretical study, *Vacuum* 12 (2016) 252–258.
- [36] Z. Jiang, T. Fang, Insight into the promotion effect of pre-covered X (C: N and O) atoms on the dissociation of water on Cu(111) surface: a DFT study, *Appl. Surf. Sci.* 376 (2016) 219–226.
- [37] W. Wang, G. Wang, Theoretical study of direct versus oxygen-assisted water dissociation on the Cu(110) surface, *Appl. Surf. Sci.* 351 (2013) 846–852.
- [38] S.L. Liu, X.X. Tian, T. Wang, X.D. Wen, Y.W. Li, J.G. Wang, H.J. Jiao, Coverage dependent water dissociative adsorption on the clean and O-precovered Fe(111) surfaces, *J. Phys. Chem. C* 119 (2015) 11714–11724.

- [39] S. Meng, E.G. Wang, S.W. Gao, Water adsorption on metal surfaces: a general picture from density functional theory studies, *Phys. Rev. B* 69 (2004), 195404-1-13.
- [40] A. Michaelides, Simulating ice nucleation one molecule at a time, with the 'DFT microscope', *Faraday Discuss.* 136 (2007) 287–297.
- [41] A. Michaelides, K. Morgenstern, Ice nanoclusters at hydrophobic metal surfaces, *Nat. Mater.* 6 (2007) 597–601.
- [42] J. Carrasco', J. Klimeš, A. Michaelides, The role of van der Waals forces in water adsorption on metals, *J. Chem. Phys.* 138 (2013), 024708-1-9.
- [43] A.A. Gokhale, J.A. Dumesic, M. Mavrikakis, On the mechanism of low-temperature water gas shift reaction on copper, *J. Am. Chem. Soc.* 130 (2008) 1402–1414.
- [44] B. Delley, An all-electron numerical method for solving the local density functional for polyatomic molecules, *J. Chem. Phys.* 92 (1990) 508–517.
- [45] B. Delley, From molecules to solids with the Dmol³ approach, *J. Chem. Phys.* 113 (2000) 7756–7764.
- [46] J.P. Perdew, J.A. Chevary, S.H. Vosko, K.A. Jackson, M.R. Pederson, D.J. Singh, C. Fiolhais, Atoms molecules, solids, and surfaces: applications of the generalized gradient approximation for exchange and correlation, *Phys. Rev. B* 46 (1992) 6671–6687.
- [47] J.P. Perdew, K. Burke, M. Ernzerhof, Generalized gradient approximation made simple, *Phys. Rev. Lett.* 77 (1996) 3865–3868.
- [48] A. Bergner, M. Dolg, W. Küchle, H. Stoll, H. Preuß, Ab initio energy-adjusted pseudopotentials for elements of groups 13–17, *Mol. Phys.* 80 (1993) 1431–1441.
- [49] Y.Y. Wang, Y.Y. Qi, D.J. Zhang, New mechanism of the direct pathway for formic acid oxidation on Pd(111), *Comput. Theor. Chem.* 1049 (2014) 51–54.
- [50] W. Gao, J.A. Keith, J. Anton, T. Jacob, Oxidation of formic acid on the Pt(111) surface in the gas phase, *Dalton Trans.* 39 (2010) 8450–8456.
- [51] S. Grimme, J. Antony, S. Ehrlich, H. Krieg, A consistent and accurate ab initio parametrization of density functional dispersion correction (DFT-D) for the 94 elements H–Pu, *J. Chem. Phys.* 132 (2010), 154104-1-19.
- [52] J.P. Ramalho, J.R.B. Gomes, F. Illas, Accounting for van der Waals interactions between adsorbates and surfaces in density functional theory based calculations: selected examples, *RSC Adv.* 3 (2013) 13085–13100.
- [53] M. Dolg, U. Wedig, H. Stoll, H. Preuss, Energy-adjusted ab initio pseudopotentials for the first row transition elements, *J. Chem. Phys.* 86 (1987) 866–872.
- [54] L.L. Fan, L.X. Ling, B.J. Wang, R.G. Zhang, The adsorption of mercury species and catalytic oxidation of Hg0 on the metal-loaded activated carbon, *Appl. Catal. A: Gen.* 520 (2016) 13–23.
- [55] K. Honkala, A. Hellman, H. Grönbeck, Water dissociation on MgO/Ag(100): support induced stabilization or electron pairing? *J. Phys. Chem. C* 114 (2010) 7070–7075.
- [56] Z.Y. Tian, S.L. Dong, Yttrium dispersion on capped carbon nanotube: promising materials for hydrogen storage applications, *Int. J. Hydrogen Energ.* 41 (2016) 1053–1059.
- [57] N.J. Govind, M. Petersen, G. Fitzgerald, D. King-Smith, J. Andzelm, A generalized synchronous transit method for transition state location, *Comput. Mater. Sci.* 28 (2003) 250–258.
- [58] L. Grabow, M. Mavrikakis, Mechanism of methanol synthesis on Cu through CO₂ and CO hydrogenation, *ACS Catal.* 1 (2011) 365–384.
- [59] J.L.C. Fajin, F. Illas, J.R.B. Gomes, Effect of the exchange-correlation potential and of surface relaxation on the description of the H₂O dissociation on Cu(111), *J. Chem. Phys.* 130 (2009), 224702-01-08.
- [60] F.J.E. Scheijen, D.C. Ferre, J.W. Niemantsverdriet, Adsorption and dissociation of CO on body-centered cubic transition metals and alloys: effect of coverage and scaling relations, *J. Phys. Chem. C* 113 (2009) 11041–11049.
- [61] W.W. Xie, L. Peng, D.L. Peng, F.L. Gu, J. Liu, Processes of H₂ adsorption on Fe(110) surface: a density functional theory study, *Appl. Surf. Sci.* 296 (2014) 47–52.
- [62] F.J.E. Scheijen, J.W. Niemantsverdriet, D.C. Ferre, Density functional theory study of CO adsorption and dissociation on molybdenum (100), *J. Phys. Chem. C* 111 (2007) 13473–13480.
- [63] S. Haq, C. Clay, G.R. Darling, G.R. Darling, A. Hodgson, Growth of intact water ice on Ru^{“0001...”} between 140 and 160 K: experiment and density-functional theory calculations, *Phys. Rev. B* 73 (2006), 115414-1-11.
- [64] S.L. Liu, X.X. Tian, T. Wang, X.D. Wen, Y.W. Li, J.G. Wang, H.J. Jiao, High coverage water aggregation and dissociation on Fe(100): a computational analysis, *J. Phys. Chem. C* 118 (2014) 26139–26154.
- [65] S. Kandoi, A.A. Gokhale, L.C. Grabow, J.A. Dumesic, M. Mavrikakis, Why Au and Cu are more selective than Pt for preferential oxidation of CO at low temperature, *Catal. Lett.* 93 (2004) 93–100.
- [66] J.L. Nie, H.Y. Xiao, X.T. Zu, First-principles study of H adsorption on and absorption in Cu(111) surface, *Chem. Phys.* 321 (2006) 48–54.
- [67] K. Gundersen, B. Hammer, K.W. Jacobsen, J.K. Nørskov, J.S. Lin, V. Milman, Chemisorption and vibration of hydrogen on Cu(111), *Surf. Sci.* 285 (1993) 27–30.
- [68] C.L.A. Lamont, B.N.J. Persson, G.P. Williams, Dynamics of atomic adsorbates: hydrogen on Cu(111), *Chem. Phys. Lett.* 243 (1995) 429–434.
- [69] J. Strömquist, L. Bengtsson, M. Persson, B. Hammer, The dynamics of H absorption in and adsorption on Cu(111), *Surf. Sci.* 397 (1998) 382–394.
- [70] K. Nobuhara, H. Nakaniishi, H. Kasai, A. Okiji, Interactions of atomic hydrogen with Cu(111) Pt(111), and Pd(111), *J. Appl. Phys.* 88 (2000) 6897–6901.
- [71] G. Lee, E. Plummer, High-resolution electron energy loss spectroscopy study on chemisorption of hydrogen on Cu(111), *Surf. Sci.* 498 (2002) 229–236.
- [72] L.H. Dubois, Oxygen chemisorption and cuprous oxide formation on Cu(111): a high resolution EELS study, *Surf. Sci.* 119 (1982) 399–410.
- [73] J. Haase, H.J. Kuhn, Reconstruction and relaxation of the oxygen-covered Cu(111) surface: a sexafs study, *Surf. Sci.* 203 (1988) L695–L699.
- [74] X.K. Gu, W.X. Li, First-principles study on the origin of the different selectivities for methanol steam reforming on Cu(111) and Pd(111), *J. Phys. Chem. C* 114 (2010) 21539–21547.
- [75] A.A. Phatak, W.N. Delgass, F.H. Ridbeiro, W.F. Schneider, Density functional theory comparison of water dissociation steps on Cu, Au Ni, Pd, and Pt, *J. Phys. Chem. C* 113 (2009) 7269–7276.